A Hyperspectral Camera in the UVA Band

A hyperspectral camera in the UVA band

Massimo Zucco, Valentina Caricato, Andrea Egidi, and Marco Pisani

***Abstract*— We present a hyperspectral camera based on a Fabry-Pérot interferometer designed to work in the UVA range (315 nm – 400 nm). The measured hypercube contains about 400 x 400 pixels, for a total of 160 000 spectra. Each spectrum has a spectral resolution of about 5 nm at the wavelength of 315 nm. Spatial and spectral discrimination capability has been demonstrated by imaging a target with five different UV emitting LEDs. Spectral resolution is demonstrated by aiming at the sky and observing spectral features of the diffused solar light in the UV. A possible application of the hyperspectral camera is the measurement of the UVA content of the diffused light of the whole sky.**

***Index Terms*—Fabry-Pérot, Fourier transforms, hyperspectral imaging, measurements techniques, optical device, spectral analysis, ultraviolet imaging, ultraviolet spectroscopy.**

I. Introduction

THE ultraviolet (UV) component of the solar radiation that reaches the Earth's surface has important effects on human health. UV radiation covers the wavelength range 100 nm – 400 nm and it is divided in three bands: UVC (100 nm - 280 nm), UVB (280 nm - 315 nm) and UVA (315 nm - 400 nm). All UVC and approximately 90 % of UVB are absorbed by ozone, water vapor, oxygen and carbon dioxide [1], then from 290 nm to about 340 nm there is an abrupt change of about five orders of magnitude in transmittance of the atmosphere and for wavelengths longer than 340 nm there is very little absorption in the atmosphere. The physiological effects of UV on life are of utmost relevance; on one hand UV radiation is detrimental since it damages deoxyribonucleic acid (DNA) molecules and some proteins of living organisms, causing skin cancers and cataracts. On the other hand, UV radiation is essential for the production of vitamin D and it is used to treat several diseases, including rickets, psoriasis and eczema [1].

To be properly protected from this harmful radiation, it is relevant to know that in the UV band the amount of radiation diffused by the atmosphere becomes important, and therefore also in the shade we can receive a harmful level of diffused light. More in details, two scattering phenomena are involved: the scattering from molecules (Rayleigh) and the scattering from the aerosol (Mie). Since Rayleigh scattering depends on the fourth power of the inverse wavelength, the diffused light increases in the UV band, and it could well exceed 70 % of the incoming solar radiation, depending on wavelength, solar zenith angle, and the amount of scattering elements in the atmosphere [2].

The global solar UV Index (UVI) gives an indication of the induced risk for human health by UV radiation. It is defined as the intensity of the radiation from 250 nm to 400 nm reaching the Earth's surface weighted with the reference action spectrum (i.e. spectral response of a biological effect) for UV-induced erythema on the human skin defined by the International Commission on Illumination (CIE) [3]. UVI is normalized in order to be a dimensionless number and is open-ended, ranging from 0 to about 10 in middle latitudes, corresponding to the highest level of risk. The UVI is obtained either by the UV spectrum measured with spectrometers weighted with the reference action spectrum or by using broadband calibrated detectors that give directly the UVI at the output.

In order to compare UVI measured by different laboratories and in different countries, it is important to have accurate and repeatable instruments traceable to the SI system. Different studies have been carried out to compare different UV radiometers, in [4] it has been showed that half of the instruments of the comparison campaign agreed within 5% and in [5] it has been showed that the relative uncertainty of a calibration is of the order of 5%. A detailed study of the uncertainty budget components is presented in [6] where all the different contributions are considered (radiometric calibration, cosine error, spectral resolution, wavelength misalignment, stability and non-linearity). Different groups and projects are active in the world in the study of the traceability of UV spectrophotometers. In particular a project funded by the European Metrology Research Programme (EMRP) is aimed at enhancing the reliability of spectral solar UV radiation in the wavelength range 300 nm to 400 nm measured at the Earth's surface by developing new methods of observation (techniques and devices) to provide traceable solar UV irradiance measurements with an uncertainty of less than 2 % [7]. Different National Metrological Institutes (NMI), laboratories and industries are involved in this project called EMRP ENV03 for "Traceability for surface spectral solar ultraviolet radiation". Amongst the issues tackled by the project there is the limited accuracy of commercial radiometers used to evaluate the UVI. One of the recognized causes of this limit is due to the design of the entrance optics;

This work was partly funded by the Project "Traceability for surface spectral solar ultraviolet radiation" EMRP ENV03.

Massimo Zucco is with the Istituto Nazionale di Ricerca Metrologica, Torino, Italy (e-mail: m.zucco@inrim.it).

Valentina Caricato is with the Istituto Nazionale di Ricerca Metrologica, Torino, Italy (e-mail: v.caricato@inrim.it).

Andrea Egidi is with the Istituto Nazionale di Ricerca Metrologica, Torino, Italy, (e-mail: a.egidi@inrim.it).

Marco Pisani is with the Istituto Nazionale di Ricerca Metrologica, Torino, Italy, (e-mail: m.pisani@inrim.it).

because such instruments measure a single spectrum of the UV light collected by an integration optical system from the whole sky. In fact the non-ideal behavior of the integration optics causes errors in the UVI estimation. Furthermore these devices cannot take into account the non-uniformity of the sky emissivity (e.g. due to the presence of clouds), causing not negligible errors. These errors can be corrected by using models which in turn need accurate and complete spectro-goniometric information of the sky emissivity. In the framework of this project we have realized a hyperspectral imager based on a Fabry-Perot (F-P) interferometer to acquire hyperspectral images in UVA band. This is an extension of the hyperspectral imager we developed to work from 400 nm to 1700 nm [8, 9] and anticipated in [10]. This prototype acquires a video of a portion of the sky and extracts the spectrum of each pixel of the image with a resolution of 12.6 THz in frequency (corresponding to about 5 nm at 315 nm). The hypercube contains about 400 x 400 pixels, for a total of 160.000 spectra. The measured portion of the sky was limited by the angle of view of the objective used in the prototype. With a UV fisheye objective it will be possible in the future to increase the portion of the monitored sky. The limit at 315 nm is due to the transmittance of the glass substrate of the semi-reflective mirrors of the F-P interferometer. We have also tested the hyperspectral imager with the spectra produced by LEDs in the UV and compared with success with the spectra measured by a spectrophotometer.

II. Theory

The different prototypes of hyperspectral imager (HSI) that we have realized are based on F-P interferometers to be inserted in an optical system where the image of a scene is formed on a camera. Then the interferograms for each pixel are extracted from the acquired video while the retardation of the interferometer is scanned by moving the mirrors from contact to a maximal distance L. The calibration of the retardation is obtained by shining the image with a laser radiation of known wavelength. Unlike Michelson interferometers where the interferogram is double-sided, Fabry-Perot interferometers produce single-sided interferograms and the retardation does not start from zero when the mirrors comes into contact as a consequence of the penetration depth in the reflective layer. The spectrum is calculated by a Fourier transform based algorithm. Furthermore, since the interferograms are based on Airy functions, as in (1), harmonics of the baseband spectrum are present in the spectrum. The harmonics decrease at the rate R^N/N where R is the reflectivity and N the order of the harmonic [11]. The harmonics of the baseband spectrum then foldover and overlap the baseband spectrum when the reflectivity R is too high. The solution we adopted in our prototypes is to use semi-reflective mirrors with a sufficient low reflectivity (R < 25%) to approximate the Airy function with a cosine function, as in (1), where d is the retardation, or optical path delay, and $\tilde{\nu}$ is the wavenumber.

$$I(\delta) = \frac{1}{1 + \left(\frac{4R}{(1-R)^2} \right) \sin^2(2\pi\, \tilde{\nu}\, d)} \approx \frac{1}{2R} + 2R\cos(4\pi\, \tilde{\nu}\, d) \tag{1}$$

Considering the sampled interferogram $I[n\Delta s]$ at the sampling interval of retardation $n\Delta s$, the formula to calculate the spectrum S, for low reflectivity mirrors and taking into account the dispersion in the phase correction Θ at the wavenumber $m\,\Delta\tilde{\nu}$ is reported in (2):

$$S[m\,\Delta\tilde{\nu}] = \left[\sum_{n=0}^{N-1} I[n\,\Delta s] \cos(2\pi\, m\,\Delta\tilde{\nu}\, n\,\Delta s) \right] \cos\left(\Theta(m\,\Delta\tilde{\nu})\right) + \\ + \left[\sum_{n=0}^{N-1} I[n\,\Delta s] \sin(2\pi\, m\,\Delta\tilde{\nu}\, n\,\Delta s) \right] \sin\left(\Theta(m\,\Delta\tilde{\nu})\right) \tag{2}$$

The sums in (2) start from 0 corresponding to the position of zero retardation, but since there is the penetration depth of the semi-reflective layer, the first terms of the sums cannot be measured and are estimated from a-priori knowledge of the regions where the spectrum is zero [8]. For the applications with the metallic mirror F-P interferometers in the 400 nm – 1700 nm range, the dispersion change is small and the calculation of S in (2) can be simplified with equation:

$$S[m\,\Delta\tilde{\nu}] = \sum_{n=0}^{N-1} I[n\,\Delta s] \cos(2\pi\, m\,\Delta\tilde{\nu}\, n\,\Delta s) \tag{3}$$

On the contrary, the dispersion change is large and strongly wavelength dependent for dielectric mirrors and for metallic mirrors for wavelength smaller than 400 nm and Θ has to be measured and corrected in order to calculate the spectrum S with (2).

III. Results

The advantage of our set-up, compared to other hyperspectral technologies, is that our F-P interferometer can be inserted in any optical set-up where the image of a target is formed on a CCD camera. The set-up shown in Fig 1 is formed, starting from the left, by the CCD camera, the F-P interferometer and the objective to form the image on the camera. The beam splitter, the diffuser and the reference laser placed in front of the objective are used for the calibration of the retardation. Our prototypes of HSI based on metallic mirrors have been tested with success in the 400 nm to 1700 nm range to produce hyperspectral cubes with applications in thermal imaging [9], spectrometry [8] and multi-labelled fluorescence microscopy [12]. In order to extend its use to UV bands, we have used the following components: a CCD camera with 12 bit resolution and 300 -1000 nm range (Pixelfly PCO), an UV objective made from quartz lenses coated with MgF_2 (UKA) and for the

retardation calibration a diode laser at 405 nm (Roithner). As anticipated in the introduction, the limit at 315 nm is due to the transmittance of the substrate of the semireflective mirrors. The uncertainty of the wavelength axis of the spectra is related to the uncertainty of the reference laser at 405 nm, that in this application is about 1 nm. The dynamic range of the measured spectra is better than 12 bits and is related to the resolution of the converter and to the oversampling of the acquisition of the interferograms.

A. Characterization of the F-P interferometer in the 315 nm – 800 nm band

In order to extend the application of the HSI to UV bands we have to characterize the dispersion and the reflectivity of the mirrors to know the correction to be put into the algorithm based on the Fourier transform (2) used to calculate the spectra.

The phase Θ has been measured with the technique explained in details in [11] where a broad-spectrum lamp with UV components, like a Xenon lamp, shines the F-P interferometer and the transmitted spectra are recorded by a spectrometer (Ocean Optics HR4000) while the distance between the mirrors is changed. From the analysis of the interferograms extracted from the succession of the spectra it is possible to fit the Airy function in (1) and extract the reflectivity $R(\lambda)$ and the dispersion phase $\Theta(\lambda)$ as a function of the wavelength and an estimation of the penetration depth of the mirrors.

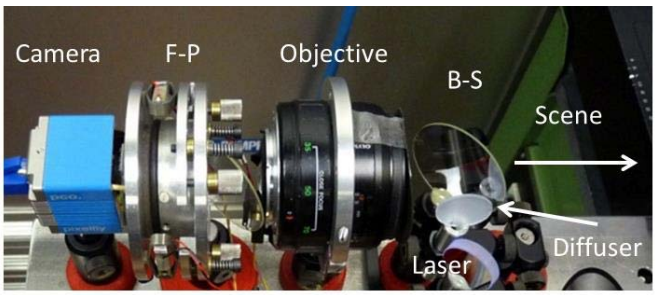

Fig. 1. Picture of a typical set-up for HSI with F-P interferometer. From the left the CCD camera, the F-P interferometer, the objective to form the image on the camera. The beam-splitter (B-S), the diffuser and the laser to calibrate the retardation.

In Fig. 2 the black line is the measured phase correction $\Theta(\lambda)$ as a function of the wavelength, the red squares are the results of a second type of measurement of Θ carried out by measuring the spectra of 7 narrow band sources with the F-P interferometer inserted in the HSI set-up. We have considered five LEDs (at maximal wavelengths of 345 nm, 355 nm, 375 nm, 396 nm and 397 nm) and two lasers (633 nm and 532 nm). The phase is relative to the wavelength 405 nm of the reference laser.

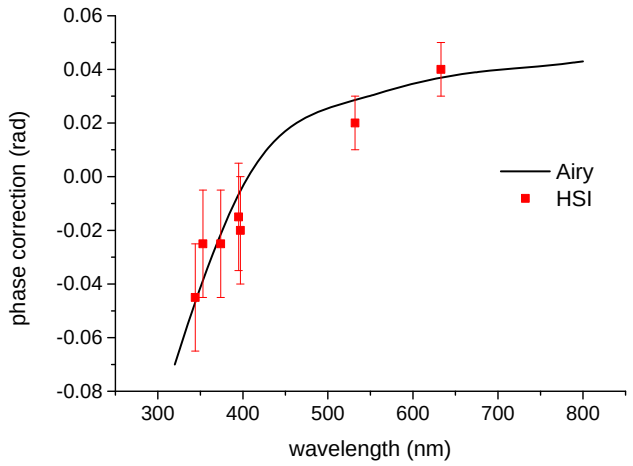

Fig. 2. Phase correction in reflection of the single metallic mirror inserted in the F-P interferometer. The black line is the measured phase correction Θ as a function of wavelength for metallic mirrors obtained by fitting the interferograms (measured with a spectrophotometer) with Airy functions. The 7 red squares are the phase corrections Θ measured using the HSI with the set-up in Fig. 1 with two lasers (532 nm and 633 nm) and five LEDs (at maximal wavelength of 345 nm, 355 nm, 375 nm, 396 nm and 397 nm).

The measured reflectivity R of metallic mirror in the F-P interferometer is reported in Fig. 3. Since R is below 25 %, we can state that the harmonics of the base spectrum will be negligible in the calculation of the spectra S [11].

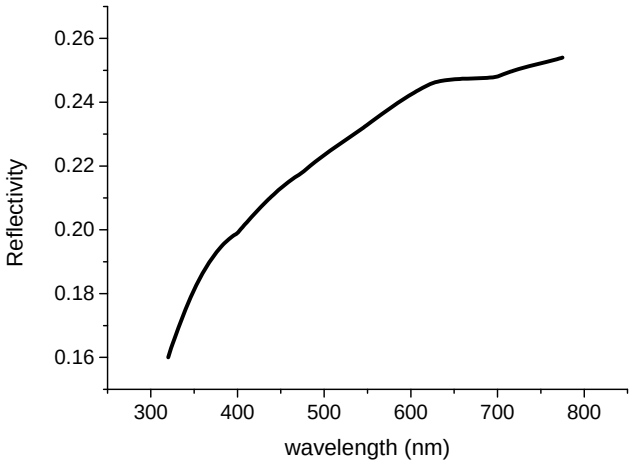

Fig. 3. Reflectivity R of the metallic mirror in the F-P interferometer measured by fitting the interferograms with Airy functions measured with a spectrophotometer.

The measurement of the penetration depth gives about 45 nm.

B. Hyperspectra of LEDs in the UVA band

As a first application we have used the HSI, with the phase correction $\Theta(\lambda)$ from Fig. 2, to acquire the hyperspectral cube of a scene containing the same five LEDs used in previous section for the characterization of the F-P interferometer. As a reference for the calibration of the retardation we have used a laser at 405 nm.

The set-up is similar to the set-up in Fig. 1 but using the

objective suitable for UV application mentioned at the beginning of the section. The results are reported in Fig. 4 where the red lines represent the normalized spectra of four LEDs at 345 nm, 355 nm, 375 nm and 397 nm extracted from the acquired hyperspectral cube. These spectra were acquired with a maximal distance between the mirrors of 24 μm, by applying a Hanning window the resolution is 12.6 THz, corresponding to about 5 nm at the wavelength of 315 nm. We compared these spectra with the ones acquired by a different spectrophotometer: in black the normalized spectra measured with a spectrometer HR4000 which has a resolution of about 1 nm. All the spectra have been normalized for comparison. The difference in the width of the spectra is due to the different resolution of the two spectrometers.

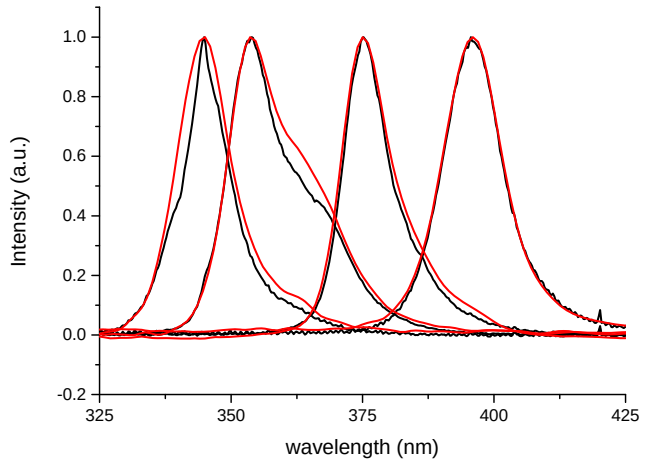

Fig. 4. In red the spectra of the radiation from four different LEDs extracted from the HSI hypercube. In black the same LED radiation measured with a reference spectrophotometer.

In order to evaluate the resolution of our HSI, the comparison of the spectra of the LEDs having the maximum at 396 and at 397 nm, measured with the two techniques, is reported in Fig. 5. The tiny difference between the two spectra can be appreciated.

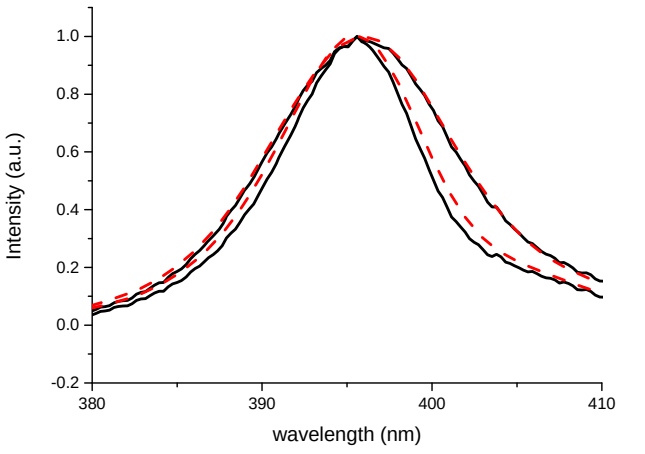

Fig. 5. In dashed red the spectra of radiation from two LEDs with the maximum at 396 nm and 397 nm In solid black the same LED radiation measured with a reference spectrophotometer.

In Fig 6 a frame of the target containing the five LEDs extracted from the video acquired during the retardation scanning.

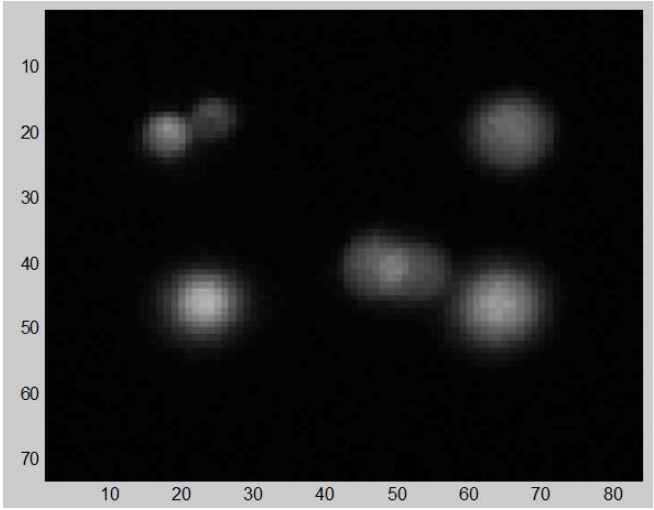

Fig. 6. Frame of the target containing the five LEDs extracted from the video while the retardation is scanned

In Fig 7 the false color image of the target with the five LEDs extracted from the hypercube using the weighing functions reported in the inset in the bottom left part of Fig 7, corresponding to two Gaussian functions centered at 350 nm, 370nm and 390 nm, with a standard deviation of 11 nm. Some LEDs appear larger due to the reflection of the LEDs on the support.

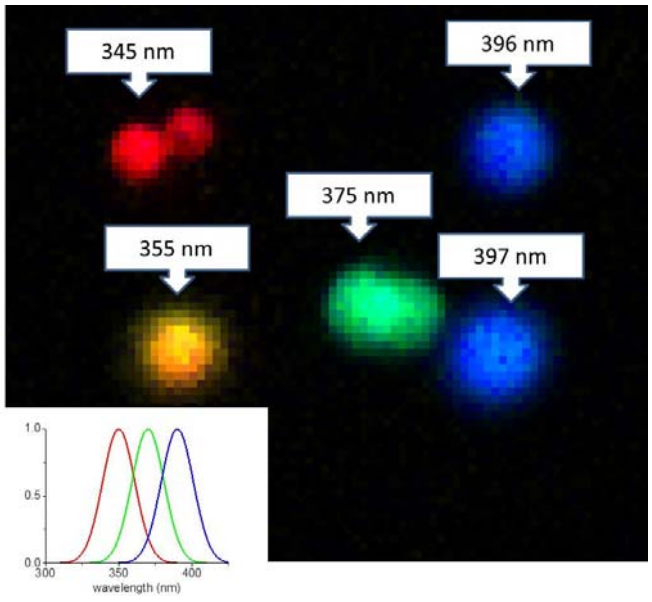

Fig. 7. False color image of the target with the five LEDs extracted from the hypercube using the weighing functions reported in the inset in the bottom left part of the figure. LEDs at 345 nm and 375 nm have collimating optics and their images appear doubled.

C. *Hyperspectra of the sky in the UVA band*

HSI has been used to measure the spectra of the sky. The picture of the set-up with the portion of the sky measured with the HSI is presented in Fig 8.

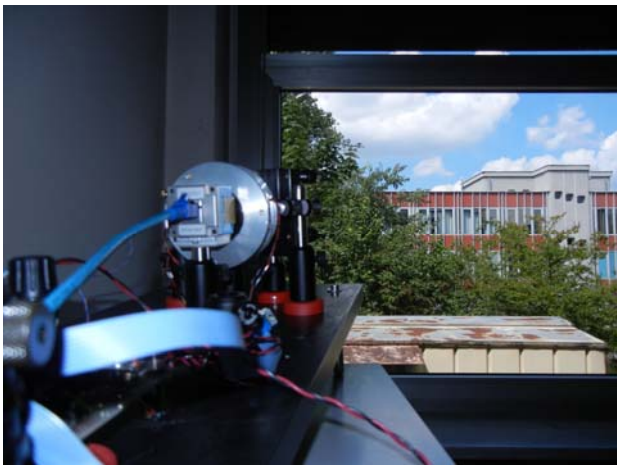

Fig. 8. A picture of the portion of the sky measured with the HSI and the set-up of HSI.

The effective angle of view of 40° of the optical system is imposed by the UV objective and by the region of contact of the F-P interferometer and is reported in Fig 9.

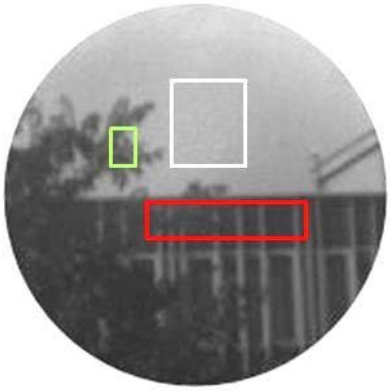

Fig. 9. Frame of the scene measured with the HSI. The white area contains portion of the sky whose spectrum is reported in Fig 10. The green and red areas contain leaves and wall whose spectra are reported in in Fig 11.

The spectrum of the sky enclosed in the white area is reported in Fig 10. The Fraunhofer lines of the solar spectrum due to the absorption of the elements present in the outer layers of the sun are clearly visible in the spectrum of the sky. These lines have a width of about 5 nm corresponding to the resolution of the spectrometer. The spectrum has to be weighed with the transmittance of all the components of the optical systems, and it could be normalized by using a reference spectrum. An optical filter cuts wavelengths higher than 500 nm.

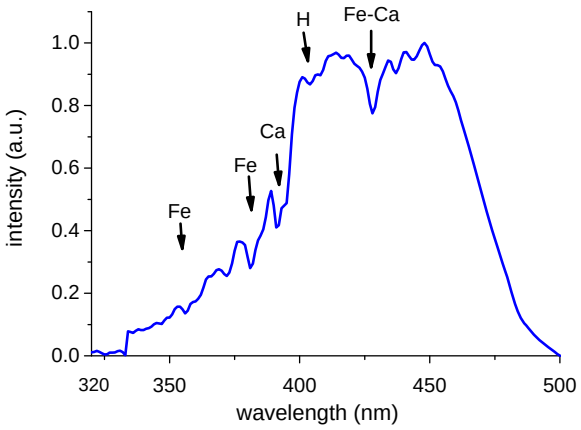

Fig. 10. Spectrum extracted from the hypercube of the diffused radiation from the portion of sky. An optical filter cuts wavelengths higher than 500 nm. Fraunhofer lines from the spectrum of the sun are indicated in the spectrum with the symbol of the element.

The spectra reflected by the leaves and by the wall of the building (green and red areas) extracted from the hypercube are reported in Fig 11.

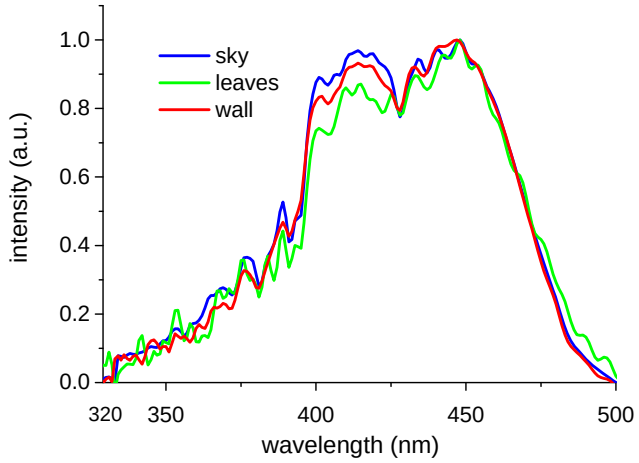

Fig. 11. Spectra extracted from the hypercube of the areas in Fig 9. The blue curve is the radiation diffused by the sky in the white area. The green and red curves represent the radiation reflected by the leaves and by the wall.

IV. Conclusion

We have realized a hyperspectral camera designed to work in the UVA range (315-400 nm). The hyperspectral camera measures a hyperspectral image made of 160,000 spectra with 5 nm resolution at 315 nm. Spatial and spectral discrimination capability has been demonstrated by imaging a target with five different UV emitting LEDs. Spectral resolution is demonstrated by aiming at the sky and observing spectral features of the diffused solar light in the UV. One of the possible applications is the integration of the UV hyperspectral camera in a fisheye optics in order to record the

whole sky diffused light in the UV. Such instrument will allow improving traceability of commercial UV radiometers which measure a single spectrum of the light collected by an integration optical system. A further improvement of the hyperspectral camera will be the implementation of a F-P interferometer with UV transparent mirrors (e.g. quartz or CaF_2) to extend the measurement range below the 315 nm limit.

ACKNOWLEDGMENT

The authors would like to thank Dr. Julian Gröbner for his help in correcting the introduction of the paper.

REFERENCES

[1] Global Solar UV Index : A Practical Guide, World Health Organization, 2002. Available: http://www.who.int/uv/publications/en/UVIGuide.pdf.

[2] A. V. Parisi, A. Green and M. G. Kimlin, "Diffuse solar UV radiation and implications for preventing human eye damage", *Photochemistry and photobiology*, vol. 73, no. 2, pp. 135-139, Feb. 2001.

[3] Erythema reference action spectrum and standard erythema dose, ISO 17166:1999/CIE S 007/E-1998

[4] A. F. Bais et al, "SUSPEN intercomparison of ultraviolet spectroradiometers." *Journal of Geophysical Research*, vol. 106, no. D12, pp. 12509-12525, Jun. 2001.

[5] G. Hülsen et al, "Intercomparison of erythemal broadband radiometers calibrated by seven UV calibration facilities in Europe and the USA." *Atmospheric Chemistry and Physics,* vol. 8, no. 16, pp. 4865-4875, 2008.

[6] G. Bernhard and G. Seckmeyer, "Uncertainty of measurements of spectral solar UV irradiance," *Journal of Geophysical Research,* vol. 104, no. D12, pp. 14321–14345, Jun. 1999.

[7] http://www.euramet.org/fileadmin/docs/EMRP/JRP/JRP_Summaries_2010/ENV03_Publishable_JRP_Summary.pdf

[8] M. Pisani and M. Zucco, "Compact imaging spectrometer combining Fourier transform spectroscopy with a Fabry-Perot interferometer", *Optics express*, vol. 17, no. 10, pp. 8319-8331, May 2009.

[9] M. Pisani, P. Bianco, M. Zucco, "Hyperspectral imaging for thermal analysis and remote gas sensing in the short wave infrared", *Applied Physics B*, vol. 108, no. 1, pp. 231-236, Apr. 2012.

[10] V. Caricato, A. Egidi, M. Pisani, M. Zucco and M. Zangirolami, "A device for hyperspectral imaging in the UV", in *Proc. CPEM*, Rio De Janeiro, Brazil, Aug. 2014.

[11] M. Zucco, M. Pisani, V. Caricato, and A. Egidi, "A hyperspectral imager based on a Fabry-Perot interferometer with dielectric mirrors," *Optics Express,* vol. 22, pp. 1824-1834, Jan 2014.

[12] M. Pisani and M. Zucco, "Fabry–Perot-based Fourier-transform hyperspectral imaging allows multi-labeled fluorescence analysis", *Applied Optics*, vol. 53, no. 14, pp. 2983-2987, 2014.

Massimo Zucco Massimo Zucco was born in Turin, Italy, in 1964. He received the degree in physics from University of Turin, in 1990 and the Ph.D degree from Politecnico of Turin, in 1995. From 1991 to 1996, he worked at IMGC-CNR. From 1996 to 1997, he worked at the NPL, Teddington, U.K., as a Research Fellow on the realization of the caesium fountain. From 1998 to 2002, he worked at IMGC-CNR to carry out concentration and spectroscopic parameter measurements. From 2002 to 2006, he worked at the BIPM, Sevres, France, on absolute optical frequency measurements using femtosecond comb techniques and on laser metrology. Since 2006, he has had a permanent position at INRIM, where he has been working on laser standards for the realization of the definition of the meter and on hyperspectral imaging.

Valentina Caricato was born in Turin, Italy, in 1977. She received the M.S. degree in physics from University of Turin in 2006 and the Ph.D. degree in physics from Politecnico di Torino in 2010. From 2010 to 2011, she was a Full Professor of mathematics and physics courses for undergraduate students at St. John International University, Vinovo, Turin, Italy. Since 2012, she has been a Post Doc Researcher at INRIM, Turin, to work in hyperspectral imaging applications in fluorescence microscopy and in spectral measurements of the UV-sky radiance. She is co-author of peer-reviewed papers on *Optic Express*, *Europhysics Letters* and *SPIE*.

Andrea Egidi was born in Narni, Italy, in 1979. He received the M.S. degree in physics at University of Perugia, Italy, in 2007. From 2008 to 2011, he was involved in several collaborations with steel/metallurgic factories, engaged in engineering and production aspects (thermal processes and design). From 2011 he was employed in an engineering company, working in R&D sector on projects based on composite materials, and in the design of photovoltaic systems. From 2012 he is a research fellow in INRIM, Turin, Italy, to work in the development of hyperspectral devices, especially in the UV, and in the development of interfeometers for space applications. He is co-author of peer-reviewed papers on *Optic Express.*

Marco Pisani was born in Milan, Italy, in 1963. He received the degree in physics from University of Turin, in 1990 and the Ph.D degree in metrology from Politecnico di Torino, in 1994. Since 1991 is with the Nationl Institute of Metrological Research (INRIM) [former Istituto di Metrologia Gustavo Colonnetti-(IMGC-CNR)] first as a PhD student then as Post Doc and as researcher since 1996. His main interests span from laser spectroscopy, interferometry, electronics, mechanical measurements and microscopy to hyperspectral imaging. Since 2013 he is Senior Researcher at INRIM.